

RESEARCH ARTICLE

Open Access



A label-free logic gate hairpin aptasensor for sensitive detection of ATP based on graphene oxide and PicoGreen dye

Jingjing Zhang, Handan Xu, Chunhui Li, Yilin Wang, Debing Liu* and Shenghe Zhao*

Abstract

Background: In this paper, a simple, enzyme-free, label-free fluorescence, high sensitivity logic gate hairpin aptasensor was developed for adenosine triphosphate (ATP) detection based on graphene oxide (GO) and PicoGreen dye.

Methods: Using single-strand deoxyribonucleic acid (DNA) and adenosine triphosphate (ATP) as input signal and fluorescence signal as output signal, if single-strand DNA (DNA-L), single-strand DNA (DNA-S), and ATP were present at the same time, one segment of DNA-L formed a hairpin ring with ATP, and the other segment of DNA-L formed a completely complementary hairpin stem with DNA-S. The hairpin DNA was detached from the GO surface, and PicoGreen dye was embedded into the hairpin stem, and the fluorescence signal was enhanced. The molecular logic gate was constructed through the establishment of logic histogram, logic circuit, truth table, and logic formula. The biosensor-related performances including sensitivity, selectivity, and linearity were investigated, respectively.

Results: We have successfully constructed a AND logic gate. The detection limit of ATP is 138.0 pmol/L ($3\sigma/\text{slope}$) with detection range of 50–500 nmol/L ($R^2 = 0.98951$), and its sensitivity is 4.748×10^6 – 6.875×10^8 a.u. (mol/L) $^{-1}$.

Conclusions: The logic gate hairpin aptamer sensor has the advantages of high sensitivity, low detection limit, and low cost, and can be successfully applied to the detection of adenosine triphosphate (ATP) in actual human urine samples.

Keywords: Aptasensor, ATP detection, Molecular logic gate, Label-free fluorescence, Enzyme-free

Introduction

Adenosine triphosphate (ATP) is associated with hypoglycemia, Parkinson's disease, hypoxia, and ischemia (Aw and Jones 1985; Agardh et al. 1978; Katsura et al. 1993). Consequently, the study of ATP detection method has important clinical significance. With high selectivity and sensitivity (Xiao et al. 2015), fluorescent biosensors have been widely used in the detection of nucleic acids, ions, proteins, and organic molecules (Li et al. 2017; Qiu et al. 2013; Wang et al. 2015).

The signal amplification and background signal suppression are two main strategies for improving DNA fluorescence sensors sensitivity. Common methods based on signal amplification can effectively increase sensor sensitivity, including rolling circle replication (RCR) (Zhou et al. 2015), strand displacement amplification (SDA) (Chen et al. 2016; Wang et al. 2013; Wei et al. 2016; Wang et al. 2017), and DNA enzymes (Zeng et al. 2015; Lu et al. 2010; He et al. 2017; Ning et al. 2017), etc. But the strategy used in these literatures requires DNA enzymes. The price of DNA enzyme is relatively high in practical application, and it is easily affected by pH and reaction temperature.

* Correspondence: 990326@hainanu.edu.cn; 180033@hainanu.edu.cn
College of Applied Science and Technology, Hainan University, Danzhou
571737, China

Compared with signal amplification strategies used in above literatures, suppressing the background signal strategies can design sensor with a simpler structure and needs a shorter reaction time (Liu et al. 2015; Lv et al. 2015). The quencher, such as gold nanoparticles (Jin et al. 2009; Yin et al. 2010), graphene oxide (GO) (Liu et al. 2015; Lv et al. 2015; Luo et al. 2018), metal-organic frameworks (Hai et al. 2018), and magnetic nanoparticles (Saberli et al. 2018), can inhibit the background signal to increase sensor sensitivity. But these approaches usually involve fluorescence-labeled probe, resulting in relatively high cost of detection. Therefore, label-free fluorescence strategies are favored by scholars. Fluorescent dye probes, such as those based on dyes thiazole orange (TO) (Kang et al. 2016), PicoGreen (Dragan et al. 2010; Lv et al. 2013) and SYBR Green I (Pu et al. 2012), and Thioflavin T (Liu et al. 2017; Song et al. 2017), have proved to be effective label-free fluorescence methods. However, neither signal suppression nor signal amplification was applied in most of these label-free fluorescence methods. In this work, we investigated the use of GO and PicoGreen dye to construct a biosensor for ATP based on enzyme-free and label-free fluorescence.

Molecular computer is of substantial significance in nanotechnology, medicine, and biotechnology. DNA logic gates can perform Boolean operations and are the hardware basis of DNA computers. Till now, many DNA logic gates, such as INH + NINH, INHIBIT, AND-NOT-AND-OR, and AND (Lv et al. 2015; Voelcker et al. 2008; Zhang et al. 2018a; Li et al. 2011), have been established. Although many molecular logic gates have been developed, there is still a need to construct logic gates that are more simple, sensitive, and less expensive. In this work, we constructed an AND logic gate based on label-free fluorescence using GO and PicoGreen, which is enzyme-free, simple, and highly sensitive.

Experimental

Reagents

The reagents and DNA sequences are shown in Tables 1 and 2, respectively. All reagents were performed in buffer solution (10 mM Tris, 10 mM MgCl₂, 50 mM NaCl, pH 7.5, and deionized water). DNA-L and DNA-S were heated for 5 min at 95 °C, and were then stored at 4 °C in a refrigerator, respectively. PicoGreen dye (200-fold dilution) and GO (100-fold dilution) were stored in a refrigerator at 4 °C. In all experiments, the volumes of DNA-L, DNA-S, PicoGreen dye, GO, and buffer solution

Table 1 Reagents

Name of reagents	Corporate name
Adenosine triphosphate (ATP)	Shanghai Yi Sheng Technology Co., Ltd. (China)
Uridine triphosphate (UTP)	
Cytidine triphosphate (CTP)	
Guanosine triphosphate (GTP)	
PicoGreen dsDNA dye	
oligonucleotides	Beijing Genomics Institute (China)
Graphene oxide (GO) sol (GO content: 1wt%)	Shanghai Aladdin Biochemical Technology Co., Ltd. (China)
Other materials	Beijing Lian Shi Yun Shang Network Technology Co., Ltd. (China)

were 30 μL, 30 μL, 20 μL, 10 μL, 1800 μL, respectively.

Before each experiment, the reagents and buffer were placed in a 2-mL sample tube, and the reaction mixture was kept for at least 24 h at room temperature.

Apparatus

Reaction times and fluorescence spectra were tested by a fluorescence spectrometer (Shimadzu, Osaka, Japan, Model: RF-6000). The wavelengths of emission and excitation used in fluorescence spectra were 480 nm and 520 nm, respectively. The emission wavelength used in the scanning spectrum was 480 nm.

Recovery of ATP in urine

Urine samples were provided by volunteers and centrifuged for 3 min at 13,000 r/min. Then, the supernatant of the centrifuged sample was diluted to 10 times with pH value of 7.5. The ATP was added in diluted samples at concentrations of 100 nM, 300 nM, and 500 nM, respectively. Each sample measurement was repeated in triplicate to compute the recovery.

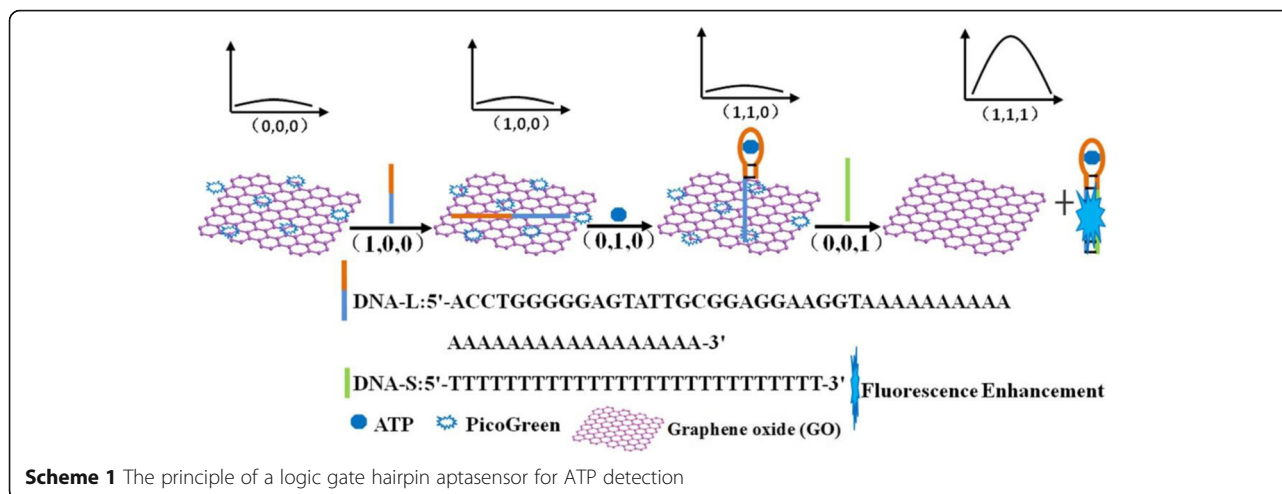
Results and discussion

The principle of a logic gate hairpin aptasensor

When the emission spectrum of the donor fluorescence molecule overlaps with the absorption spectrum of the receptor fluorescence molecule, and the distance between the two molecules is less than a

Table 2 DNA sequences

Name	DNA sequence
DNA-L	5'-ACCTG GGGGA GTATT GCGGA GGAAG GT AAAAA AAAAA AAAAA AAAAA AAAAA AA-3'
DNA-S	5'- TTTT TTTT TTTT TTTT TTTT TT-3'

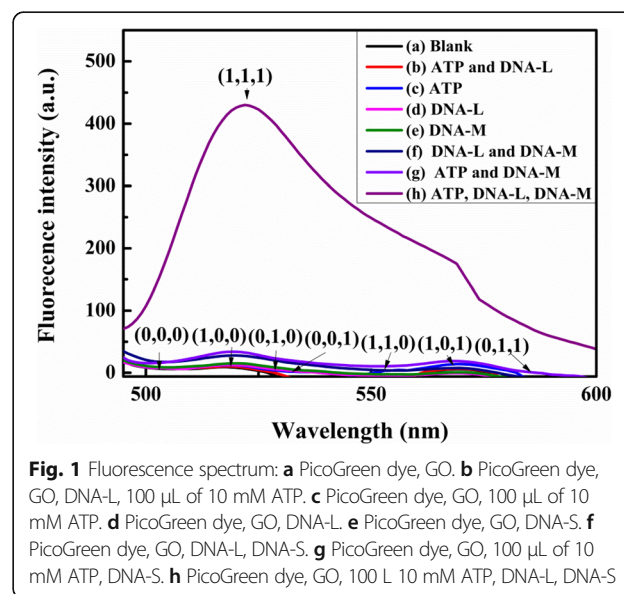


certain distance, the fluorescence energy will transfer from the donor to the receptor. If the fluorescence quantum yield of the acceptor is zero, the fluorescence resonance energy transfer (FRET) will lead to fluorescence extinction. In this work, PicoGreen fluorescence molecule was used as energy donor and GO as energy receptor. Single-stranded DNA was adsorbed on the surface of GO through π - π stacking, fluorescence resonance energy transfer (FRET) occurred between PicoGreen dye combined with single-stranded DNA and GO, and fluorescence was quenched. But double-stranded DNA with perfect pairing did not have this property (Zhang et al. 2018a; Li et al. 2011; Zhang et al. 2018b; Zhang et al. 2018c). Scheme 1 exhibits the principle of an aptasensor for ATP detection. In the presence of a single-strand DNA (DNA-L), fluorescence was quenched because DNA-L was adsorbed on the surface of GO, resulting in FRET. When ATP was added, the ATP aptamer (the red fragment in DNA-L) formed a hairpin with ATP, and another fragment (the blue fragment in DNA-L) adsorbed on GO, resulting in fluorescence quenching. When a single-strand (DNA-S) was added, it paired with blue fragment in DNA-L to form complementary hairpin double-stranded DNA. The hairpin double-stranded had a weak binding force with GO, and it detached from the GO. The distance between PicoGreen embedded in double-stranded DNA and GO increased, and FRET could not occur between PicoGreen and GO. The fluorescence was significantly enhanced, thus achieving the purpose of ATP detection. If DNA-L, ATP, and DNA-S were taken as input signals and fluorescence as output signals, this principle conformed to AND logic operation law. In this

principle, the PicoGreen dye was used to construct a label-free and enzyme-free hairpin aptasensor, and the GO inhibited the fluorescence background signal generated by the binding of incomplete paired hairpin double stranded DNA, which was beneficial to improve the sensitivity of the sensor.

Mechanism feasibility verification

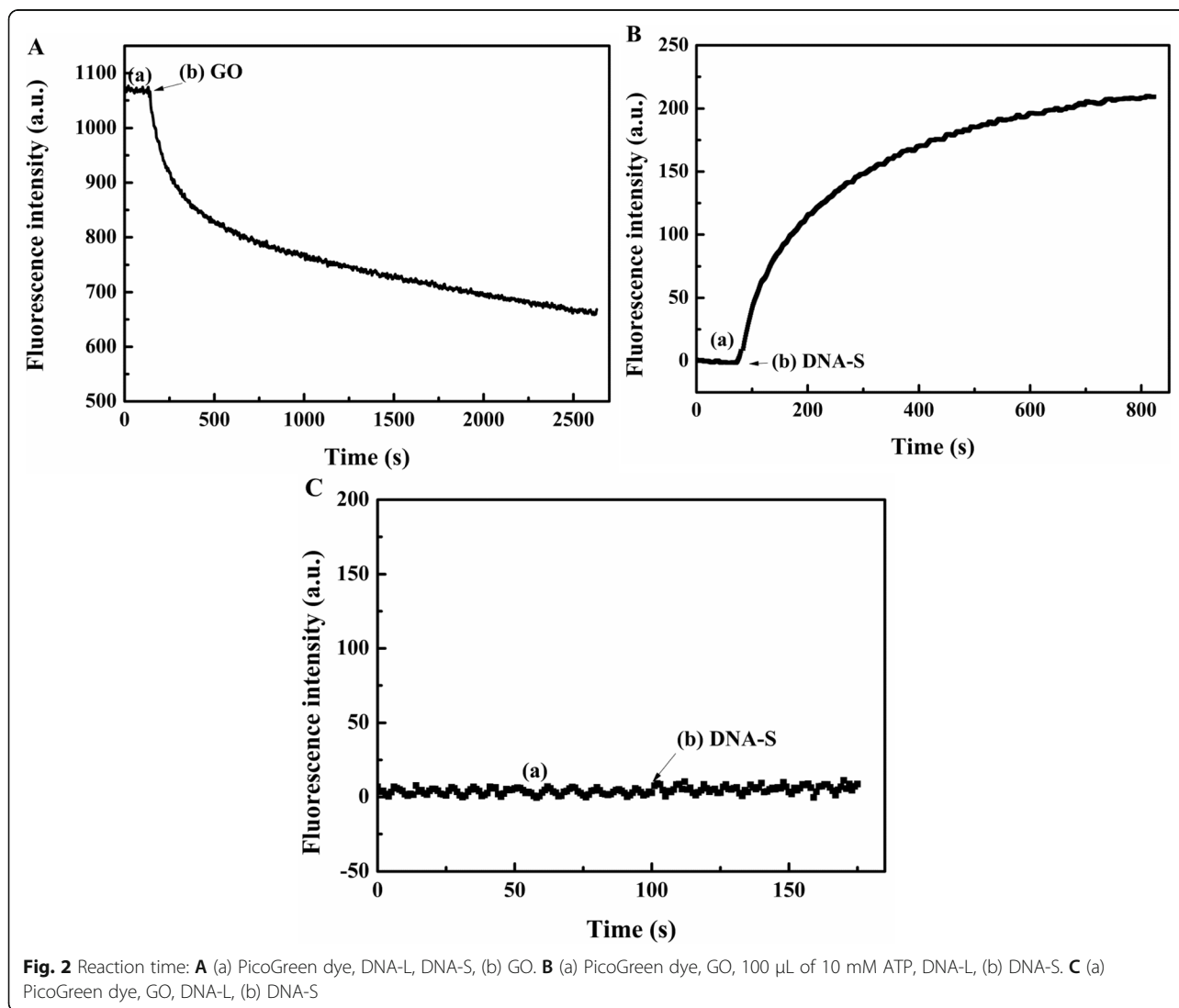
Figure 1 exhibits that the fluorescence signals (a- to g-curve vs. h-curve) were relatively weak because of the adsorption of single-stranded DNA on the GO surface, leading to FRET. The h-curve fluorescence signal was obviously enhanced. Because ATP aptamer



segment in DNA-L formed a hairpin structure with ATP, and the A-based segment in DNA-L was completely paired with DNA-S, resulting in double-stranded hairpin DNA shedding from GO surface. PicoGreen interacted with double-stranded DNA (DNA-S + DNA-L) to produce more obvious fluorescence signals. It shows that the 3:1 logic gate is feasible for use in detection of ATP.

The purpose of the following experiments was to further verify the correctness of the principle. Figure 2A shows that when GO was added to mixed solutions, the fluorescence signal rapidly decreased because of the adsorption of single-stranded DNA on the GO surface, leading to FRET. This result was consistent with the result of the a-curve (see Fig. 1). Figure 2B demonstrates that the fluorescence signal is enhanced in

the presence of DNA-L, DNA-S, and ATP. Because ATP aptamer segment in DNA-L formed a hairpin structure with ATP and the A-based segment in DNA-L was completely paired with DNA-S to form dsDNA (DNA-L+DNA-S), falling off the GO surface. And then PicoGreen interacted with dsDNA (DNA-S + DNA-L) to produce more obvious fluorescence signal which also demonstrates the result of h-curve (see Fig. 1). Figure 3c shows that the fluorescence signal does not change in the presence of DNL-L and DNA-S. Because DNL-L and DNA-S are paired to form double stranded DNA (DNL-L + DNA-S) with sticky ends, which were adsorbed on the GO surface, resulting in FRET and fluorescence quenching. These results further prove that of f-curve shown in Fig. 1. In summary, the results in Fig. 2



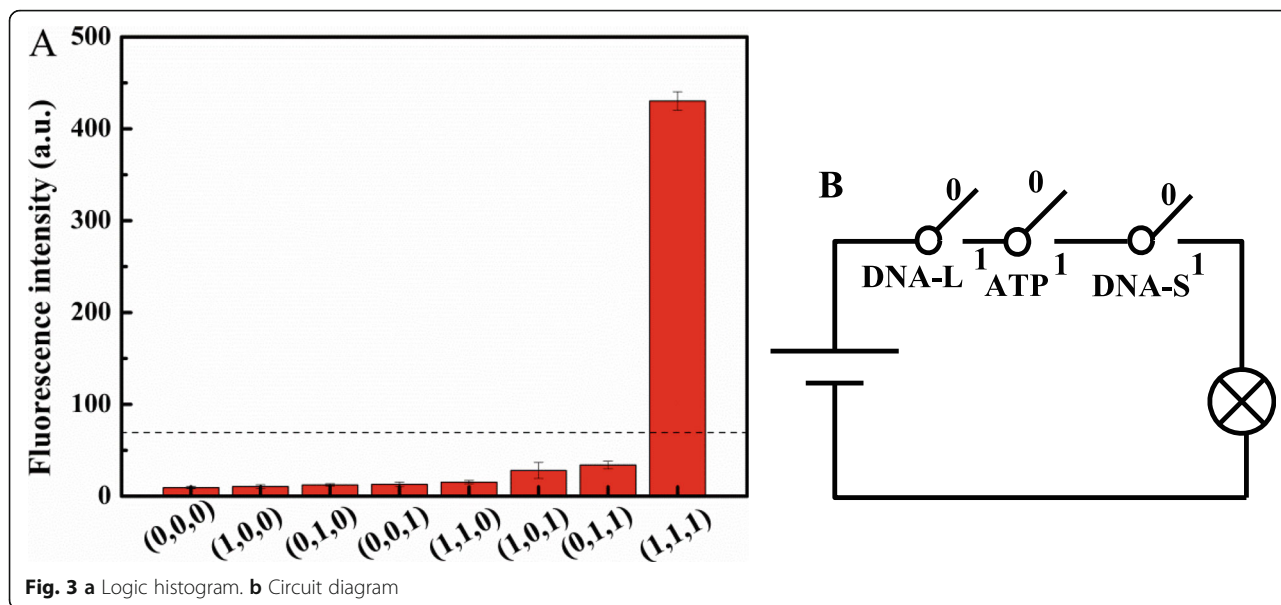


Fig. 3 a Logic histogram. b Circuit diagram

are consistent with those described in Fig. 1, which further verifies that the principle of the 3:1 logic gate is feasible.

Construction of DNA logic

If DNA-L, DNA-S, or ATP exits, the input signal of logic gate is 1, if not, the input signal is 0, labeled as (DNA-L, ATP, DNA-S). Meanwhile, when the fluorescence change, ΔF , is greater than 50 a.u., the output signal of logic gate is 1, otherwise it is 0. The fluorescence change value is $\Delta F = F - F_0$, where F_0 is the a-curve peak value, and F is the other curves (b- to h-curve) peak value (see Fig. 1). According to the result of Fig. 1, the logic bar chart is drawn, as shown in Fig. 3a. Figure 3a exhibits that DNA-L, ATP, and DNA-S coexist (1,1,1), the fluorescence intensity changes significantly. Using to the

Table 3 Truth table

$I_1 = (\text{DNA-L})$	$I_2 = (\text{ATP})$	$I_3 = (\text{DNA-S})$	Out
0	0	0	0
0	0	1	0
0	1	0	0
0	1	1	0
1	0	0	0
1	0	1	0
1	1	0	0
1	1	1	1

results of Fig. 3a, the DNA circuit is constructed as shown in Fig. 3b.

According to Fig. 3 results, the truth table is constructed (Table 3). Using the truth Table 3, the following can be deduced:

$$Out = I_1 \cdot I_2 \cdot I_3 \tag{1}$$

A three input single output (3:1) AND logic gate is drawn by formula (1), as shown in Fig. 4.

Linearity and sensitivity

All the reagents were stored at 4 °C, because the conformation of DNA and ATP were stable at low temperature, which effectively improved the stability of the sensor. Figure 5a exhibits the spectral curves of different ATP concentrations. The fluorescence intensity of a-curve is taken as F_0 , and the other curve (b-, c-, d-, e-, f-, g-curve) peak is taken as F . Figure 5b is calculated based on the result of Fig. 5a. The detection range was from 50 nM to

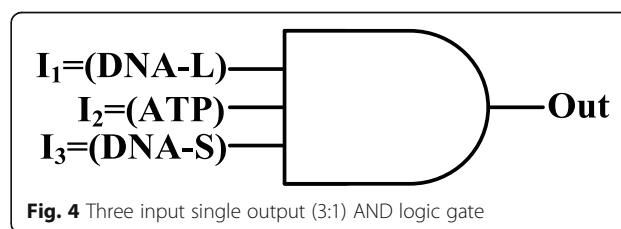
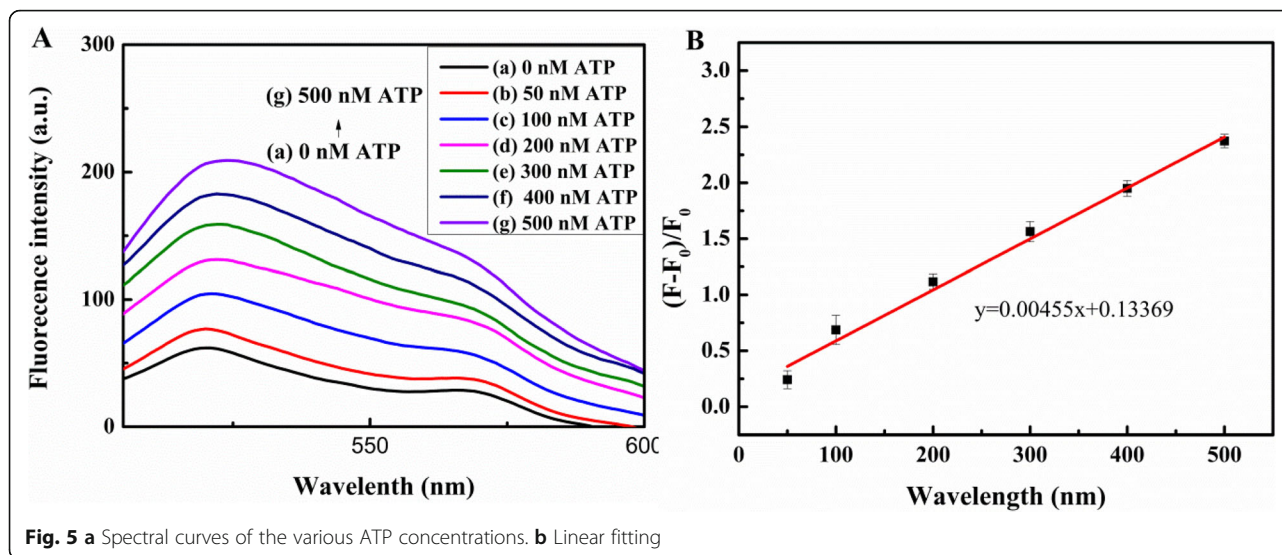


Fig. 4 Three input single output (3:1) AND logic gate



500 nM. The fitting linear equation was $y = 0.00455x + 0.13369$ ($R^2 = 0.98951$) with the detection limit of 138.0 pmol/L ($3\sigma/\text{slope}$). The results in Table 4 clearly exhibit that the proposed method has lower detection limits, sufficient linearity, and higher sensitivity compared with most other documents. The sensitivity is shown in Fig. 6 with a range of $4.748 \times 10^6 \text{ a.u.}(\text{mol/L})^{-1} - 6.875 \times 10^8 \text{ a.u.}(\text{mol/L})^{-1}$.

Table 4 Comparison of methods

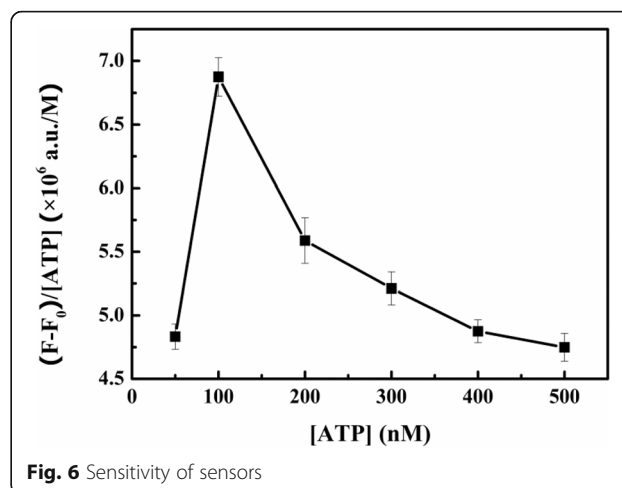
Linear range	LOD	Correlation coefficient (R^2)	Reference
100–1000 nmol/L	30 nmol/L	0.9950	(Yu et al. 2013)
0–0.5 mmol/L	8 $\mu\text{mol/L}$	–	(Lu et al. 2014)
1 nM–100 $\mu\text{mol/L}$	0.5 nmol/L	0.996	(Zhang et al. 2018d)
0.1 pM–5 nmol/L	0.1 pmol/L	0.9984	(Wang et al. 2018)
0.1–10 $\mu\text{mol/L}$	33 nmol/L	0.98	(Lee et al. 2014)
10–850 nmol/L	5.0 nmol/L	0.9901	(Mashhadizadeh et al. 2017)
0.5–8.0 $\mu\text{mol/L}$	91.6 nmol/L	0.99	(Zhu et al. 2016)
5–230 nmol/L	2.4 nmol/L	0.9854	(Shahsavari et al. 2017)
5 nmol/L–50 mmol/L	1.597 pmol/L	0.9914	(Gu et al. 2020)
20 fmol/L–100 nmol/L	20 fmol/L	0.997	(Yang et al. 2019)
50 nmol/L–5 mmol/L	2 nmol/L	0.996	(Ma et al. 2019)
50–500 nmol/L	138.0 pmol/L	0.98951	This work

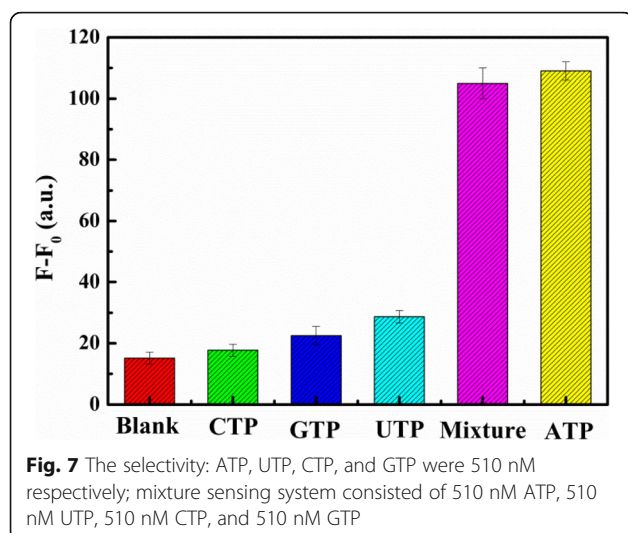
Specificity

In order to evaluate the specificity of the sensor, the similar molecules (CTP, UTP, and GTP) was tested by the proposed method. All reagents were stored in refrigerator at 4 °C to maintain the conformation of DNA and the performance of reagents (ATP, CTP, UTP, and GTP). Figure 7 exhibits that compared with the similar molecules (CTP, UTP, and GTP), fluorescence signal increased significantly in the presence of the target ATP. In addition, there was no significant difference between the fluorescence signals caused by mixture and ATP alone. These results clearly prove that this method has enough specificity.

Detection of ATP in real sample

The purpose of recovery test is to verify the practical application performance of the sensor. Table 5 shows that





the 3:1 AND logic gate has good recoveries in the range of 97.54–108.04%, indicating that the proposed method exhibits immense potential for ATP detection in human urine.

Conclusions

We have developed a logic gate hairpin aptasensor for sensitivity detection of ATP. This 3:1 AND logic gate has many advantages. First, the GO suppresses the background signal to improve sensitivity. Second, the proposed assay does not require enzymes or fluorescent labeling, thus reducing the cost of analysis. Third, this method has sufficient specificity for the detection of ATP, and the detection range was from 50 to 500 nmol/L with the detection limit of 138.0 pmol/L. Finally, the recommended method successfully detects ATP in urine. As a result of above advantages, the proposed strategy can also be applied to the detection of other ions and proteins.

Table 5 ATP recovery test

Sample	ATP added (nM)	Proposed method			
		Found (nmol/L)	Recovery (%)	Standard deviation (n = 3) (nmol/L)	Relative standard (n = 3) (%)
1	100	112.98	108.04	4.38	4.06
		108.82			
		102.33			
2	200	215.01	104.89	4.02	1.91
		209.12			
		205.22			
3	300	293.12	97.54	2.43	0.83
		289.43			
		295.33			

Abbreviations

GO: Graphene oxide; FRET: Fluorescence resonance energy transfer; DNA: Deoxyribonucleic acid; dsDNA: Double-stranded deoxyribonucleic acid; DNA-L: Single-stranded deoxyribonucleic acid with the number L; DNA-S: Single-stranded deoxyribonucleic acid with the number S; ATP: Adenosine triphosphate; UTP: Uridine triphosphate; CTP: Cytidine triphosphate; GTP: Guanosine triphosphate

Acknowledgements

All the authors are very grateful for the experimental equipment provided by Hainan University, as well as the financial support provided by Hainan Provincial Education Department and Hainan University famous teachers' studio.

Authors' contributions

J.Z. wrote the paper. H.X. and C.L. performed the experiments. Y.W. analyzed the data, and D.L. and S.Z. conceived and designed the experiments. All authors read and approved the final manuscript.

Funding

This work was supported by the Key Project of Research and Development in Hainan Province (Grant No. ZDYF2020038), the Education Department of Hainan Province (Project number: Hnky2020-19; Hnky2021-18), the Famous teachers' Studio of Hainan University (Grant No. hdms202022), the Natural Science Foundation of Hainan Province (Grant No. 119MS001), and the Educational and Teaching Reform Research Project of Hainan University (Grant No. hdjy2074; Grant No. hdjy2106).

Availability of data and materials

Research data have been provided in the manuscript and supporting information.

Competing interests

The authors declare no conflicts of interest.

Received: 20 October 2020 Accepted: 3 February 2021

Published online: 25 February 2021

References

- Agardh CD, Folbergrova J, Siesjo BK. Cerebral metabolic changes in profound, insulin-induced hypoglycemia, and in the recovery period following glucose administration. *J Neurochem.* 1978;31:1135–42.
- Aw TY, Jones DP. ATP concentration gradients in cytosol of liver cells during hypoxia. *Am J Physiol.* 1985;249:C385–92.
- Chen HG, Ren W, Jia J, Feng J, Gao ZF, Li NB, Luo HQ. Fluorometric detection of mutant DNA oligonucleotide based on toehold strand displacement-driving target recycling strategy and exonuclease III-assisted suppression. *Biosens Bioelectron.* 2016;77:40–5.
- Dragan AI, Casas-Finet JR, Bishop ES, Strouse RJ, Schenerman MA, Geddes CD. Characterization of PicoGreen Interaction with dsDNA and the Origin of Its Fluorescence Enhancement upon Binding. *Biophys J.* 2010;99:3010–9.
- Gu Y, Li J, Qian K, Zhang Z, Wang S, Wang J. Integrated dual-signal aptasensor based on magnet-driven operations and miniaturized analytical device for on-site analysis. *Sensors Actuators B: Chemical.* 2020;310:127856.
- Hai X-M, Li N, Wang K, Zhang Z-Q, Zhang J, Dang F-Q. A fluorescence aptasensor based on two-dimensional sheet metal-organic frameworks for monitoring adenosine triphosphate. *Anal Chim Acta.* 2018;998:60–6.
- He S, Qu L, Tan Y, Liu F, Wang Y, Zhang W, Cai Z, Mou L, Jiang Y. A fluorescent aptasensor with product-triggered amplification by exonuclease III digestion for highly sensitive ATP detection. *Analytical Methods.* 2017;9:4837–42.
- Jin Y, Li H, Bai J. Homogeneous selecting of a quadruplex-binding ligand-based gold nanoparticle fluorescence resonance energy transfer assay. *Anal Chem.* 2009;81:5709–15.
- Kang BH, Gao ZF, Li N, Shi Y, Li NB, Luo HQ. Thiazole orange as a fluorescent probe: Label-free and selective detection of silver ions based on the structural change of i-motif DNA at neutral pH. *Talanta.* 2016;156-157:141–6.
- Katsura K, Folbergrova J, Bengtsson F, Kristian T, Gido G, Siesjo BK. Recovery of mitochondrial and plasma membrane function following hypoglycemic coma: coupling of ATP synthesis, K⁺ transport, and changes in extra- and intracellular pH. *J Cereb Blood Flow Metab.* 1993;13:820–6.

